CLM - P 570

CLM - P 570

UKAEA

Preprint

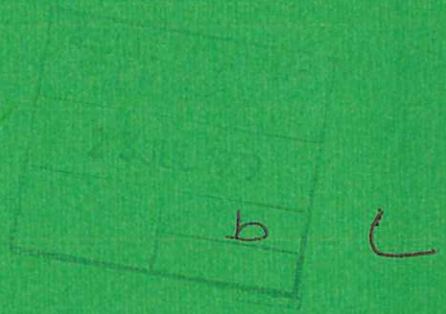

XUV EMISSION AS A DIAGNOSTIC OF LASER HEATED PLASMAS

N J PEACOCK

CULHAM LABORATORY
Abingdon Oxfordshire

1979

CLM-P 570

XUV EMISSION AS A DIAGNOSTIC OF LASER HEATED PLASMAS

by

N J Peacock
Culham Laboratory, Abingdon, Oxon. OX14 3 DB UK
(Euratom/UKAEA Fusion Association)

ABSTRACT

The emission or absorption of soft x-ray light can be used as the basis for diagnostic techniques in the compression of material in microballoons which are irradiated by intense laser light.

"Explosive-pusher" laser irradiation experiments at the University of Rochester USA and at the Rutherford Laboratory, UK, using 'slot-hole' crystal spectrometers, allow space-resolution of the XUV spectrum emitted from the compressed core, from the microballoon shell and from the ablation layer. Stark-broadened line emission from quantum states ($\overline{n} \geq 4$) of hydrogen-like Si^{13+} and O^{7+} from the glass microballoon wall, and from Ne^{9+} when neon is used as a fill gas, allow derivation of the compression ($\frac{\rho}{\rho_o}$), while the 'opacity broadening' of lower Lyman series lines allow a derivation of the confinement factor $\langle \rho R \rangle$.

At the Rutherford Laboratory, backlighting the compressed core with XUV emission ($\lambda \sim 10$ Å) from a subsidiary, irradiated target is used to follow the time history of the compression and indicates substantially similar compression factors.

The analysis of these results are critically reviewed and it is indicated in this lecture that considerable care has to be taken with the analysis of the Stark profiles especially, when at high densities, correlations, ion dynamics and Debye screening play important roles. Furthermore in the analysis of $\langle \rho R \rangle$ the equation of radiative transfer should be solved for an inhomogenous plasma with temperature gradients and differential plasma velocities.

The general area of XUV diagnostic techniques remains, however, a powerful tool in material compression experiments. The scope for x-ray analysis would be enlarged very much further however if XUV lasers were to be developed. Then the probe light might be 'frequency-tuned' to the absorption spectrum of specific diagnostic test atoms included in the compression.

(Paper presented at the International School of Plasma Physics, Course on Diagnostics for Fusion Experiments, Varenna, 4-16 September 1978. To be published in the Proceedings by Pergamon Press).

December 1978

1. INTRODUCTION

The range of diagnostic techniques used to study the extreme pressure plasmas produced in laser-compression experiments is described in some considerable detail by Coleman [1]. Since the plasma density can exceed the propagation cut-off value for most existing laser probe wavelengths, measurement techniques are favoured which make use of the short wavelength emission which escapes from and is characteristic of the dense plasma itself.

This paper describes the manner in which plasma properties can be deduced from a spectroscopic analysis of the x-ray emission. It is seen that the line and continuum emission from suitable diagnostic test ions allows one to derive the important parameters of density ρ, and therefore the volume compression, and also the fusion burn efficiency factor $\langle\rho R\rangle$. The $\langle\rho R\rangle$ value of a D, T plasma in which fusion reactions take place, is related to $n\tau$ the Lawson confinement criterion for energy break-even, viz.

$$n\tau = nR/V_{th} \simeq 5 \times 10^{14} \text{ cm}^{-3} \text{ sec}$$

Here, V_{th} is the ion thermal velocity and can be regarded as almost constant in a thermonuclear plasma with $V_{th} \simeq 10^{8}$ cm sec^{-1}. Identifying ρ with the density n, we have

$$\langle\rho R\rangle \simeq 0.2 - 0.5 \text{ gm cm}^{-2}$$

Both the parameters ρ and $\langle\rho R\rangle$ can be derived from spectral line profiles.

Spectroscopic analysis is capable of deriving much more information about the plasma however. The detailed line shapes also contain information on mass motion, thermal broadening, electron temperature gradients and magnetic field effects. The continuum emission can be interpreted directly in terms of the electron velocity distribution function. Space-resolution of the order of microns and time-resolution of the order of picoseconds are ideally required and sophisticated measurement techniques encompassing these orders of magnitude are described by Coleman [1].

In early experiments on laser irradiation of plane solid targets, spectroscopic measurements were successfully used to derive plasma parameters at or below the cut-off density n_c for laser propagation. In these experiments, Galanti and Peacock et al [2] [3]; Burgess et al al [4], the density profile of the expanding plasma 'corona' with $n_e \lesssim n_c$ ($n_c = 10^{21}$ cm^{-3} for 1.06 μm neodymium laser irradiation) has been measured from Stark broadening. Hydrogen-like ions such as C^{5+}, O^{7+} were particularly useful diagnostic ions. The plasma dimensions were also deduced both from 'opacity broadening' of the centre of the emission line profiles and from non-stationary model calculations of the relative ion populations, [2] [3]. In recent experiments on microballoon targets compressed by multiple-beam laser irradiation, these line broadening diagnostic methods have been adopted, by Yaákobi et al [5]; Bristow et al [6] and by Evans et al [7], to measure ρ and $\langle\rho R\rangle$. Typically, values of $\rho R \sim 10^{20}$ electrons cm^{-2} are attained in the compressed plasma core.

An alternative and attractive method for studying the dimensions of the compressed plasma

in symmetrically irradiated microballoon experiments uses x-ray shadowgraphy and has been reported recently by Evans et al [7].

This paper describes the physical basis for the spectroscopic analyses in these microballoon experiments. It is pointed out that existing Stark broadening data e.g. Griem [8] are not adequate to deal with ultra-dense plasmas with several component particle species. At the present time this is an active theoretical topic however. It is also emphasised in this paper that theoretical predictions of the experimental line profiles from laser-irradiated plasmas involve often complex model calculations of the radiative transfer of line emission through inhomogenous, non-stationary plasmas.

Diagnostics methods based on the relative intensities of emission lines in the x-ray region are not discussed in detail in this paper. For these analyses the reader is referred to such papers as Aglitskii et al [9]; Vinogradov et al [10], [11]; Doschek et al [12]; Peacock [13].

Review papers on spectroscopic methods for ultra-dense plasmas are relatively few. Vinogradov et al [14] were possibly the first to discuss the potential of spectroscopy as a diagnostic technique in the study of dense highly-ionised matter compressed by laser-irradiation. Peacock [13] has described the theoretical background to some topical spectroscopic experiments on various ultra-dense, laboratory plasma sources. A lucid description of the physical effects and problems in the interpretation of spectroscopic features in ultra-dense plasmas is given by Burgess [15].

2. LINE BROADENING IN LASER-COMPRESSED PLASMAS

The most intense lines in high temperature plasmas lie in the XUV or X-ray region of the spectrum. The spectral profiles of these lines are determined partly by the instrument resolution and partly by source broadening. Crystal dispersion is most frequently used in X-ray line studies and the resolving powers ($\lambda/\delta\lambda \geq 10^4$ is commonly achieved) are sufficiently high to enable the source profile to be unfolded. When an unfocused (flat) crystal is used, care has to be taken that there is no great loss in resolution due to the plasma source dimensions.

In typical experiments on the spatial analysis of laser-compressed microballoon targets rare gases such as neon are often added to the gas filling as indicators of the compression, see e.g. Key et al [16]. Diffracted light from the plasma is imaged via a narrow slit onto film or the photocathode of an x-ray streak camera. The length of the slit determines the range of diffraction angles and therefore the wavelength coverage while the width of the slit determines the spatial resolution as in figure 1. Each point in the plasma contributes to a different image point and this instrument broadening accounts for the spectral width of the Si lines from the relatively cold, outer glass plasma, figure 2. The Ne X lines from the compressed plasma core are grossly broadened by the plasma and are not materially affected by instrument broadening.

The variation in the x-ray spectrum, produced by a 0.2 TW laser pulse divided between four beams, is shown in figure 3 for various neon gas filling pressures. These experiments, Bristow et al [6] at the University of Rochester, well illustrate the potential and the difficulties of spectral analyses. A glance at figure 3 will suffice to realise that many of

the lines are asymmetric. The Ne IX $1s^2$-1s3p transitions for example has relatively more energy on its long wavelength wing than on the other wing, probably due to the presence of dielectronic satellites, Peacock [17]. Several of the lines have other weak transitions superimposed on their wings while the lower resonance series members of Ne X are seen to be self-reversed in their centre. These complications leave relatively sparse regions of the spectrum, notably the Ne X Lyman γ line, on which to perform plasma broadening analysis.

The broadening of the line within the plasma, which we will term the 'intrinsic plasma broadening,' is most often determined by Doppler shifts due to mass-motion or thermal effects. Stark broadening, for most ions, is relatively small with the very important exception of hydrogenic ions which are often used therefore as diagnostic indicators of the density. Magnetic field effects in the x-ray region can normally be neglected also although for very large, multi-megagauss fields and at longer wavelengths this assertion will not hold. Zeeman splitting is of the order

$$\Delta\lambda_z = g\ K\ \lambda^2\ B_M \qquad (1)$$

where $K = 4.7 \times 10^{-5}$ cm^{-1}; and $\Delta\lambda_z$ is of the order ~ 0.05 Å for $B_M = 10^7$ G and a wavelength $\lambda = 100$ Å.

Opacity effects, which if severe may result in saturation or even reversal of the spectral core of the emission line can cause an apparent broadening of the line. This is not to be thought of as true intrinsic broadening however but is more a property of the plasma dimensions and its temperature structure. The effects of opacity are most marked for resonance transitions involving the heavily populated ground-state of the ion.

Following these preliminary remarks, the discussion in the following sections will be centred around firstly Stark broadening, since its analysis leads directly to the plasma density, and secondly opacity since from this we may derive the parameter $\langle\rho R\rangle$.

3. DENSITY MEASUREMENTS FROM LINE BROADENING

Linear Stark broadening of degenerate hydrogen-like ions is by far the most significant effect of density on line shapes and it is the most readily estimated. Vinogradove et al [14] points out that over a range of charge states from Z=1→25 and a complementary range of density from $10^{18} \rightarrow 10^{23}$ cm^{-3} the broadening of the wings of the lines will be due to quasi-static ion microfields, Griem [8]. Broadening by electrons will affect mainly the line centres due to impact mechanisms, Griem [8] up to $n_e \sim 10^{25}$ cm^{-3}.

Curve fitting over only a limited part of the line profile, where opacity, Stark shifts and mass-motions are operative, is notoriously unreliable. Also singular measurements of only the half intensity widths of the lines can be misleading, firstly due to intensity saturation or reversal in optically thick situations and secondly due to strong undisplaced central components in the Stark pattern such as is the case for Lyman α, γ. Ideally therefore we should like to fit the total experimental profile to a family of theoretical profiles calculated over a range of plasma parameters. Unfortunately no comprehensive data, such as exists for H^o, He^{+1} at lower densities Griem [8], are available to describe Stark profiles of hydrogenic ions immersed in a high temperature, multi-component plasma at densities in excess

of 10^{21} cm^{-3}. There are however, several levels of sophistication which one might adopt in order to provide an answer.

In a very rudimentary fashion, a mean Stark shift may be derived from

$$- \Delta\omega_{if} (\bar{E}) = C_{if}\bar{F} \tag{2}$$

where $C_{if} \simeq (3\hbar/2emZ) (n_i^2 - n_f^2)$ are the Stark coefficients for initial and final quantum states, n_i and n_f; $\bar{F}$ is the mean quasi-static particle field,

$$\bar{F} = 8.8 \, z_p \, e \, N_p^{2/3} \tag{3}$$

where N_p is the perturber density and z_p is the charge on the perturber ion species. Generally it is assumed $\Sigma Z N_p = N_e$. For a transition, such as Ly β, with no unshifted central stark component, and identifying $C_{if}\bar{F}$ as the half width, Griem [8] derives for the half width of the optically thin line,

$$\Delta\omega = (12 \, z_p \hbar/Zm) (n_i^2 - n_f^2) N_p^{2/3} \tag{4}$$

Expressions for the electron impact broadening of the central components of the Ly α, Ly γ lines are given by Yaákobi et al [18] and by Griem [19].

A sounder approach however is to compare the experimental profile with the full theoretical line profiles incorporating both ion and electron effects. These latter are usually calculated in terms of S(α) for various values of α, with α in Å/CGS units of field strength.

Data which will allow the simple construction of the full Stark broadened profiles have been tabulated only for low charge states H^o and He^+, at low temperatures of a few eV and for densities $\leq 10^{20}$ cm^{-3}, see Griem [8]. One might make a tentative use of this data however to give some indication of the Stark profiles at higher density and for higher charge states provided the values of the spectral shift α, are suitably reduced by Z^{-5} (from eq. 2 and 4) and provided that the perturber charge is taken into account in the definition of the field strength (eq.6).

For extended profile fits to the line wings only, a simple Holtsmark quasi-static ion microfield distribution, Griem [8], may be used. At very high densities however there are two main corrections to this distribution. The first, which becomes important when the screening parameter 'a' → 1 is due to the screening of the ions by the electrons. This effect causes a reduction in the microfield and therefore in the broadening.

$$'a' = \frac{r_o}{\lambda_D} = \frac{8.3 \times 10^{-4} \, N_e^{\frac{1}{2}}}{N_z^{1/3} (kTe)^{\frac{1}{2}}} \tag{5}$$

where kTe is in eV, r_o is the ion-ion separation and λ_D is the Debye length. The Holtsmark distribution is generally written W(β), where W(β) is the electric microfield distribution as

a function of $\beta = F/F_o$, and F_o is the 'normal' Holtsmark field,

$$F_o = 2.603\, \bar{z}_p\, e\, N_p^{2/3} \qquad (6)$$

Strictly, Holtsmark only applies for 'a' $\to 0$, i.e. in the high temperature, low density limit. At the other extreme with a$\sim$1 the distribution predicted by 'nearest neighbour theory', would apply. These microfield distributions are plotted by Mihalas [20] and Hooper [21], for example. At values of β much higher than we expect to deal with, the asymptotic form of $W(\beta)$ for both of these distributions is approximately the same i.e. $W(\beta) = \frac{3}{2}\, \beta^{-5/2}$. In laser compression experiments 'a' lies typically between $\sim$ 0.1 and 1.0 so that Debye screening corrections are important.

A second correction to Holtsmark fields at high densities is required for correlations between emitters and perturbers. The criterion for this correction to be significant is that the correlation length, λ_{ZZ_p} is $\geq r_o$, the interparticle separation, i.e.,

$$\lambda_{ZZ_p} = \frac{(Z-1)Z_p\, e^2}{kTe}\ , \text{ and } N_p \geq [kTe/(Z-1)\bar{z}_p\, e^2]^3 \qquad (7)$$

For a plasma with mean charge Z=10 and kTe = 100 for example, eq.(7) requires the perturber density $N_p > 4 \times 10^{20}$ cm^{-3}.

Accurate microfield distributions $W(\beta)$, taking into account both screening and radiator-perturber correlations, have been calculated by Hooper [21] for a range of 'a' parameters. The effect of correlations for the case of a two-component plasma has been considered by O'Brien and Hooper [22]. Very few calculations exist however for multiple component plasmas at high density; but see Tighe and Hooper [23]. Smith and Peacock [24] point out that Hoopers' microfield distributions are more generally useful and practically became independent of the perturber charge when r_o in eq.(5) is defined as the mean perturber separation r_p rather than the electron separation r_e.

Once the microfield distribution $W(\beta)$ has been calculated the intensity of the emission at any frequency ν is given by

$$L(\nu)d\nu = W(\beta)d\beta \quad \text{i.e. } L(\nu) = \frac{k}{CF_o}\, W(\beta) \qquad (8)$$

where C is the Stark coefficient, see e.g. Underhill and Waddell [25]; k is a normalisation constant which takes into account the fractional oscillator strength of the Stark-shifted component; for Ly α, for example, $k = \frac{1}{6}$.

Within the last few years numerical codes have been constructed which will predict the <u>total</u> line profile of highly-stripped, hydrogenic ions in ultra-dense plasmas. These codes, Richards [26]; Tighe and Hooper [23], include electron impact and static ion effects corrected, using Hooper's formalism, Hooper [21], for some correlation effects and Debye screening. The results of these computations have indeed been used with substantial success

for the analysis of density in laser irradiated target-plasmas, Galanti and Peacock et al [2] Yaákobi et al [18], see for example figure 4. The presentation of the theoretical data from these complex codes in any general form which is useful to the experimentalist is a problem however, and published data exists for only a few specific ions in very specific plasma conditions. The lower Lyman series profiles of Ne X, Al XIII and Ar XVIII have been published by Tighe and Hooper [23] for N_e 1→2 x 10^{23} cm^{-3}, see also Yaákobi et al [18], while Lee [27] has published data for Ne X and Si XIV in nearly the same plasma conditions. Examples of these theoretical profiles are shown in figures 5 and 6.

4. <ρR> FROM OPTICALLY THICK LINES

In the case of the intense optically thick lines there is a problem in normalising the experimental core intensity to the theoretical profile. Yaákobi et al [5] [18], have overcome this problem in microballoon compression experiments by profile-fitting simultaneously to the higher series members where these latter are optically thin and distinguishable above the continuum. An example of this analysis is shown in figure 4. Smith and Peacock [24], in their studies of laser-irradiation of plane targets, circumvent the line-centre optical depth problem by relating the intensity in the far (optically thin) wings of the line to the adjacent free-bound continuum intensity from the same ion, figure 7. For Lyman lines whose upper levels are thermally populated with respect to the free electrons, the line wing to continuum intensity ratio is a function only of the intrinsic line shape and of the electron temperature parameter, this being derived directly from the free-bound continuum slope.

Microfield distributions $W(\beta)$ were rescaled by Smith and Peacock [24] in terms of 'a' = r_p/λ_D, while suitable mean perturber charges were ascribed to each plasma condition based on the ion populations derived from relative intensities of the respective free-bound continuum steps as in figure 7. The results of curve fitting to the optically thin parts of the C^{5+} Lyman profiles are shown in figure 8. Peak electron densities of 2 x 10^{21} cm^{-3} are deduced for both PTFE and $(CH_2)_n$ target plasmas with an accuracy of ∿ 20%.

We now turn our attention to the core intensity of the optically thick lines. The solution of the radiation transfer equation gives the intensity emerging from a homogenous plasma of depth R,

$$I(\nu) = \frac{\varepsilon(\nu)}{a(\nu)} \left[1 - e^{-\tau(\nu)}\right] \qquad (9)$$

$\varepsilon(\nu)/a(\nu)$, the ratio of the emissivity of the line to its opacity at frequency ν, is termed the source function S_ν. In local thermodynamic equilibrium S_ν is given by the Planck function with the characteristic temperature of the free electrons. In plasmas produced by laser-irradiation of solids, non-stationary conditions with steep temperature gradients are common-place, Peacock [17], and S_ν will depend on the instantaneous populations of the upper and lower atomic levels.

$\tau(\nu)$ is the optical depth which is related to the intrinsic line shape $L(\nu)$ by

$$\tau(\nu) = \rho(z)\, L(\nu)\, \frac{h\nu_o}{c}\, B\, R \qquad (10)$$

B, the Einstein absorption coefficient is expressed here in terms of energy density. Alternatively

$$\tau(\nu) = \int \rho(z,R)\, f_{12}(\pi e^2/mc)\, \frac{\phi(\nu)}{\phi_o}\, .dR, \qquad (11)$$
$$\propto \langle \rho R \rangle$$

where $\phi(\nu) = \phi_o L(\nu)$ and ϕ_o is the full, half intensity width of the line; Cooper [28].

For $\tau(\nu_o) > 1$ the emission profile is flat topped in the core at ν_o. The profile remains flat (in a stationary homogeneous plasma) over a frequency range $\nu_o \pm \nu$ where $\tau(\nu) = 1$. At this frequency

$$\langle \rho(z) R \rangle = \frac{c}{L(\nu)\, h\nu_o\, B} \qquad (12)$$

The line shape $L(\nu)$ is determined by Stark, Doppler etc., broadening in the plasma.

In some microballoon irradiation experiments, Bristow et al [6]; the Ne^{9+} Lyman α emission does indeed have a flat topped profile, as in figure 9, indicating a homogeneous plasma in the compressed core. From the radiation transfer equation (eq.9) and using $L(\nu)$ derived by Tighe and Hooper [23], Bristow et al [6] can account for these profiles with an optical depth at line centre $\tau(\nu_o) \gtrsim 100$. For Lyman β of Ne^{9+} under the same experimental conditions, a best fit is found for $\tau(\nu_o) = 0.5$, figure 10. Rather similar results are reported by Evans et al [7].

Yaákobi et al [18] give an expression for $\langle \rho R \rangle$ in terms of $\tau(\nu_o)$,

$$\langle \rho R \rangle = \tau_o\, \Delta\nu_{\frac{1}{2}} \left(\frac{mM(z)\, c}{\pi e^2 f}\right) \frac{\sum_{z'}^{z''} N(z)}{N(z)} \qquad (13)$$

where $\Delta\nu_{\frac{1}{2}}$ is the full half width of the intrinsic line profile as determined by Stark and Doppler effects and the ion mass M is inserted to convert eq.(13) to gm cm^{-2}. Inserting appropriate values for $\Delta\nu_{\frac{1}{2}}$ and τ_o gives $\langle \rho R \rangle = 2.2 \times 10^{-4}$ gm cm^{-2} for the 8.6 atmosphere neon gas filling, Yaákobi et al [18]. These authors are not *a priori* entitled to assume that the flat core intensity is given by the Planck function. However in their experiments, it appears that the ratio $N(Ne^{+9})/N_e$ [$N(Ne^{+9})$ being derived from eq.(13) and $N_e = 7 \times 10^{22}$ cm^{-3}, from the Lγ profile, figure 4] is consistent with the temperature value one might expect for a Planckian temperature derived from the relative intensities of Ly α and Ly β.

More commonly in laser irradiation experiments, spatial inhomogeneities in the mass motion and in the relative level populations of the emitting and absorbing ions cause the line profiles to be shifted, and self-reversed, see e.g., Peacock [13]. Model calculations of line profiles based on solutions of the radiation transfer equation for expanding or contracting plasmas have been derived by Irons [29]. Essentially, emission lines from an optically-thick inhomogeneous plasma which is expanding and cooling will have a self-reversed core which is blue-shifted. An opposite shift of the self-reversal to the red will occur for contracting plasmas. Skupsky [30] has considered the limitations to the $\langle \rho R \rangle$ analysis from optically thick lines in laser fusion experiments when the lines are distorted due to mass

motion and temperature gradients. It is apparent that in many compression experiments a simple expression such as eq.(13) is not applicable and that fairly complex line profile modelling is required.

5. VALIDITY OF THEORETICAL LINE PROFILES

A few cautionary remarks on the validity of the theoretical line shapes in ultra-dense plasmas might not be amiss at this juncture. Calculations of the total Stark-broadened profiles used in the analysis of compression experiments e.g. Tighe and Hooper [23] can only be subjected to a quantitative test when the perturber concentrations are independently determined. So far this has not been the case. The theory of Stark broadening is, moreover, being continuously modified. Weisheit and Rozsnayai [31] point out that line shifts and asymmetries occur not only when the electrons screen the interactions between radiators and perturbers but also screen the coulomb interactions within the atomic structure of the radiating atom itself. Recent Stark broadening calculations by Lee [32] and Griem[19] include electron ion correlations and ion dynamics which lead to shifts and asymmetries in the line profiles. An interesting feature of Lees' calculations, Lee [32] is the predicted appearance of enhanced resonance effects at the ion plasma frequency.

A very useful review of the status of line broadening in ultra-dense plasmas is given by Burgess [15]. Burgess points out that Doppler narrowing of the line ought to be of some significance in high density plasmas. Suppression of the Doppler width, Dicke [33], can occur when the mean free path between collision becomes of the order of the emitted photon wavelength λ, i.e. when

$$N_p \gtrsim \left(\frac{kT}{Z_p^2 e^2}\right) \frac{\perp}{\pi\lambda} \ln\Lambda \qquad (14)$$

For $Z=Z_p=N_e/N_p=10$, Doppler narrowing should occur for $N_p \gtrsim 10^{20}$ cm^{-3} at temperatures of a few hundred eV, Burgess [15]. Line narrowing should therefore be a relatively common phenomena and ought to be an important feature of studies of opacity and stimulated emission, for example, where the absolute intensity of the line core is required. In the analysis of laser compression experiments this effect has not so far been noted perhaps because of the current emphasis on wing broadening effects.

6. PULSED X-RAY RADIOGRAPHY

We have noted that distortion of emission line shapes due to opacity can in principle be used to derive information on the concentration of the ions, their mass motion and temperature gradient, Irons [29], Skupsky [30]. This principle is carried a stage further in experiments at the Rutherford Laboratory, Evans et al [7] where the laser-drive implosion is illuminated by an external, pulsed, background continuum as illustrated in figure 11. Again neon is added as a diagnostic gas filling and absorption of the continuum by the dense, compressed neon plasma provides a straightforward radiograph of the implosion. The rate at which energy is extracted from the illuminating beam of intensity I_υ is $I_\upsilon a_\upsilon$, where a_υ is the absorption cross-section at frequency υ. For photo-absorption between bound atomic levels, 'ℓ' and 'u'

$$a_\nu = N_z(\ell).\frac{B_{\ell u}}{c} h\nu_{u\ell} L(\nu) \tag{15}$$

i.e., $$a_{\nu_o} = N_z(\ell).A_{u\ell} \frac{\lambda^2}{8\pi} \quad \frac{1}{\Delta\nu_{\frac{1}{2}}} \tag{16}$$

where $\Delta\nu_{\frac{1}{2}} \simeq (L(\nu_o))^{-1}$ is the intrinsic half-width of the line in the plasma.

If the upper level lies in the continuum, then a_ν is the photo-ionisation cross-section viz.

$$a_\nu = \frac{\pi e^2}{mc} \cdot f_{u\ell} \cdot \frac{\Delta k}{\Delta\nu} \tag{17}$$

where Δk is the number of free states with effective oscillator strength $f_{u\ell}$ in the frequency interval $\Delta\nu$. For hydrogenic ions with nuclear charge Z, the photo-absorption cross-section, Cooper [28], from level n to the free level 'v' is given by

$$\sigma_{nv}(\nu) = \frac{2^6\pi^4 e^{10} m}{3\sqrt{3}\, eh^6} \quad \frac{Z^4}{n^5} \quad \frac{g_{f-b}}{\nu^3} \tag{18}$$

g_{f-b}, the free-bound Gaunt factor is tabulated by Karsas and Latter [34]. Eq.(18) only applies to frequencies greater than that at the free-bound absorption limit i.e. $\nu > \frac{Z^2 Ry}{hn^2}$, where Ry is a Rydberg.

In the Rutherford Laboratory experiments, the spectrum of the illuminating light, produced by subsidiary laser illumination of a brass target, figure 11, is itself broad-band, with a mean energy of about 1.5 keV. This energy is less than the photo-ionisation threshold of the He-like Si and so the predominant absorption is due to oxygen and neon, probably in He-like states, at temperatures between 40 and 250 eV.

A composite sequence of pictures is shown in figure 12 where the x-ray pin-hole camera was set up to view the implosion against the background illumination. At early times < 350 ps transmission of the x-ray illumination through the core suggests an initial, shell-structure in the implosion. The almost complete absorption of the broad-band illumination is suggestive of mainly photo-ionisation processes in the later stages of the implosion. This would account for the relative insensitivity of the absorption to temperature gradients and dynamic motion.

It should be emphasised that x-ray experiments are only effective in <u>low</u> temperature compressions i.e. when the 'colour temperature' of the illumination is of the same order as, or higher than, the effective temperature of the compressed plasma; this latter being defined as

$$\frac{N_z(u)}{N_z(\ell)} = \frac{g_u}{g_\ell} \exp^{-\psi_{u\ell}/kTe} \qquad (19)$$

In higher temperature compression experiments the inherent radiated intensity from the plasma will become competitive with the background illumination while at the same time, (eq.19), the number of ions capable of absorbing in the lower ground state will decrease.

The development of a narrow-band illumination source which could be frequency-matched to bound-state energy differences in the plasma ions would result in a dramatic improvement in the flexibility of x-ray absorption techniques. Ideally the source would have a temperature higher than the effective bound state temperature eq.(19). In principle then it would be possible to identify and follow the variation in the concentration of each separate ion species during the compression. A laser system perhaps operating with the same ion species as the diagnostic test ions in the compressed plasma but with output in the XUV region would fulfill these requirements. While no such lasers exist at present, experiments on amplification of XUV light by stimulated emission, using plasma as a gain medium is a topical subject in studies of intense laser-interaction with matter.

7. ACKNOWLEDGEMENTS

The author would like to thank C C Smith, R W Lee and D D Burgess of Imperial College for useful discussions on this paper. Figures 1, 2, 11 and 12 are reproduced by permission of the Rutherford Laboratory, UK, while figures 3, 4, 9 and 10 are reproduced by permission of the Laser Energetics Laboratory, the University of Rochester, USA.

REFERENCES

[1] COLEMAN L: "Laser Fusion Diagnostics", Lectures I, II and III, Proc. Int. School of Plasma Physics, Course on Diagnostics for Fusion Experiments Varenna, 1978. Publ. by Pergamon Press, this volume.

[2] GALANTI M, PEACOCK N J, NORTON B A, PURIC J: "Light Absorption and Energy Balance at the Surface of a Laser-Irradiated Solid Target". Proc. 5th Int. Conf. on Plasma Physics and Controlled Nuclear Fusion Research, Tokyo 1974. Paper CN-33/F3-4. Publ. 1975 IAEA Vienna.

[3] GALANTI M and PEACOCK N J; "Quantitative X-ray Spectroscopy of the Light Absorption Region at the Surface of Laser-Irradiated Polyethylene". J.Phys.B. Atom.Molec. Phys. 8, No 14, pp 2427-2447, 1975.

[4] BURGESS D D, FAWCETT B C and PEACOCK N J; "Vacuum Ultraviolet Spectra from Laser-Produced Plasmas". Proc, Phys. Soc. 92, Part 3, pp 805-816, 1967.

[5] YAAKOBI B, STEEL D, THOROS E, HAUER A and PERRY B; "Direct Measurement of Compression of Laser-Imploded Targets using X-ray Spectroscopy", Phys. Rev. Lett., 39, pp 1526 - 1529 , 1977.

[6] BRISTOW T, DELETTREZ J et al; "Explosive-Pusher Type Laser Compression Experiments with Neon-filled Microballoons". Proc. 7th Int. Conf. on Plasma Physics and Controlled Nuclear Fusion Research, Innsbruck, Austria. Paper CN-37-B-4 to be published 1979, IAEA Vienna.

[7] EVANS R G, KEY M H, NICHOLAS D J et al; "Dynamics of Laser-Produced Implosions of Gas Filled Microballoon Targets". Proc. 7th Int. Conf. on Plasma Physics and Controlled Nuclear Fusion Research, Innsbruck, Austria. To be published 1979, IAEA Vienna.

[8] GRIEM H R; "Spectral Line Broadening in Plasmas". Academic Press, London and New York, 1974.

[9] AGLITSKII E V, BOIKO V A, VINOGRADOV A V, YUKOV E A; "Diagnostics of Dense Laser Plasmas Based on the Spectra of Hydrogen-like and Helium-like Multiply Charged Ions". Sov. J.Quant. Electron (Moscow), 1, pp 579-590, 1974.

[10] VINOGRADOV A V, SKOBOLEV I Yu, YUKOV E A; "Intensity Ratio of Fine Structure Components of Hydrogen-like Ions in a Dense Plasma" (Transl. Am.Inst.Phys.), Sov.J. Plasma Phys. 3, pp 389-394, 1978.

[11] VINOGRADOV A V, SKOBOLEV J Y, YUKOV E A; "Density Dependent Lines of H, He and O-like Ions in Laboratory Plasma Diagnostics", Lebedev Inst. Report No. 121, 1977.

[12] DOSCHEK G A, FELDMAN U, DAVIS J and COWAN R D: "Density Sensitive Lines of Highly-Ionised Iron", Phys. Rev. A, 12, pp 980-986, 1975.

[13] PEACOCK N J; "Spectroscopy of High Density Plasmas", Proc. Int. Conf. on Phenomena in Ionised Gases, Berlin, Vol. Invited Papers pp 383-405. Published by Physical Society of the GDR 1977. Also Culham Laboratory Report CLM-P519 (1978).

[14] VINOGRADOV A V, SOBELMAN I I and YUKOV E A; "Spectroscopic methods for Diagnostics of Superdense Hot Plasmas". Kvant.Elektron. (Moscow), 1, pp 268-278, 1974.

[15] BURGESS D D; "Spectroscopic Effects in Dense and Ultra-dense Plasmas", Symposium on Physics of Ionised Gases, (1978), Proc. of Invited Papers (Editor Janev) to be published by Inst. of Phys. Belgrade, Yugoslavia 1979.

[16] KEY M H, EVANS R G et al; "implosion and Compression of Gas-filled Microballoons", Paper IV.9, 11th Euro. Conf. on Laser Interaction with Matter, Oxford 1977. Available as Rutherford Laboratory Report, RL-77-122/B, Rutherford Laboratory, Oxon, UK.

[17] PEACOCK N J; "Spectroscopy of Highly-Stripped Ions in Laser-Induced Plasmas" in Beam Foil Spectroscopy, Editors Sellin and Pegg, Vol. 2, pp 925-950. Published by Plenum Publishing Corp. New York (1976).

[18] YAAKOBI B, STEEL D et al; "Explosive Pusher Type Laser Compression Experiments with Neon-Filled Microballoons", Laboratory for Laser Energetics Report No. 74, University of Rochester, USA. 1978.

[19] GRIEM H R: "Broadening of the Lyman α Lines of Hydrogen and Hydrogenic Ions in Dense Plasmas", Phys. Rev., 17, pp 214-217, 1978.

[20] MIHALAS D; "Stellar Atmospheres", W H Freeman & Co. 1977.

[21] HOOPER C F: "Low-frequency Component Electric Microfield Distributions in Plasmas"(I); "Asymptotic Electric Microfield Distributions in Low Frequency Component Plasmas" (II).
(I) Phys. Rev. 165, pp 215-222, 1968
(II) Phys. Rev. 169, pp 193-195, 1968

[22] O'BRIEN J T and HOOPER C J; "Low - Frequency Electric Microfield Distributions in a Plasma Containing Multiply Charged Ions", Phys. Rev. A5, No 2, pp 867-884, 1972.

[23] TIGHE R J and HOOPER C F; "Stark Broadening in Hot, Dense, Laser-Produced Plasmas, A two component, two temperature formulation". Phys. Rev. A17, pp 410-413.

[24] SMITH C C and PEACOCK N J; "Electron Density Measurements Using the Stark-Broadened Line Wings of Hydrogenic Ions in Laser-Produced Plasmas". J.Phys.B, Atom. Molec. Phys. Vol 11, No 15, pp 2749-2763, 1978.

[25] UNDERHILL A and WADDELL J; "Stark Broadening Functions for the Hydrogen Lines", NBS Circular No 603, Washington DC, US Dept. of Commerce, 1959.

[26] RICHARDS A G; "Stark profiles in High Density Multi-Component Plasmas", unpublished, 1974, but see Ref. 13 1979.

[27] LEE R W; "Study of the Plasma Broadening of Spectral Lines of Hydrogenic Ions", J.Phys.B, Atom.Molec.Phys. Accepted for publication, 1978.

[28] COOPER J: "Plasma Spectroscopy" reports in Progress in Physics XXIX, part 1, pp 35-130, 1966.

[29] IRONS F E; "Radiative Transfer across Expanding Laser-Produced Plasmas; I, line profiles; II, line intensities and stimulated emission".
I J.Phys. B Atom. Molec. Phys. 8, No 18, pp 3044-3068, 1975
II J.Phys. B Atom. Molec. Phys. 9, No 15, pp 2737-2753, 1976

[30] SKUPSKY S; "Optically Thick Spectral Lines as a Diagnostic Tool for Laser-Imploded Plasmas", Laboratory for Laser Energetics, Report No 80, University of Rochester, USA, 1978.

[31] WEISHEIT J C and ROZSNYAI B F; "On the Asymmetry of Lines Emitted by One Electron Ions in Very Dense Plasmas', J.Phys.B. Atom.Molec.Phys., 9, No.4, pp L63-67, 1976.

[32] LEE R W; "A Model Study of Non Thermal Effects in the Plasma Broadening of Spectral Lines", submitted J.Phys.B. Atom.Molec.Phys. 1978.

[33] DICKE R H; "The Effect of Collisions upon the Doppler Width of Spectral Lines", Phys. Rev. 89, pp 472-473, 1953.

[34] KARSAS W J and LATTER R: "Electron Radiative Transitions in a Loulomb Field". Astrophys. J. (suppl.) No 55, 6, pp 167 - 212, 1961.

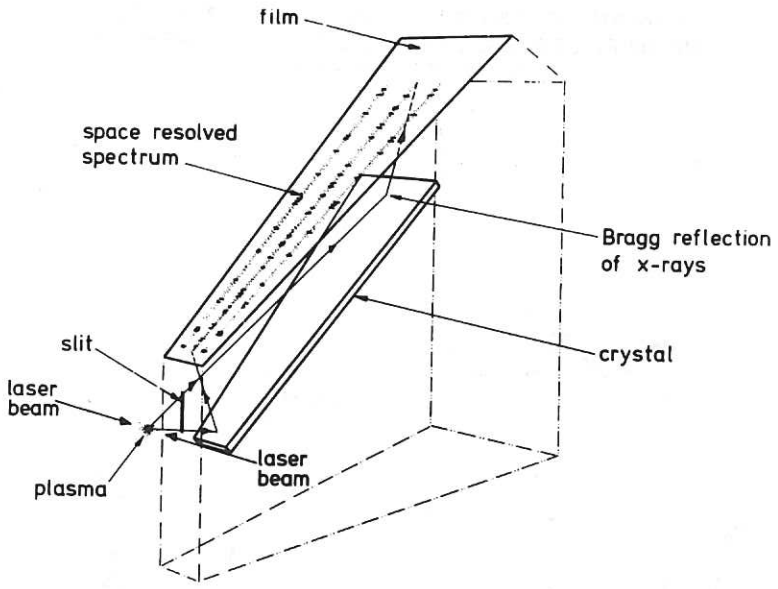

Fig.1 X-ray, flat crystal spectrometer using slit hole for space resolution of spectral emission from 2-beam laser-irradiated target.

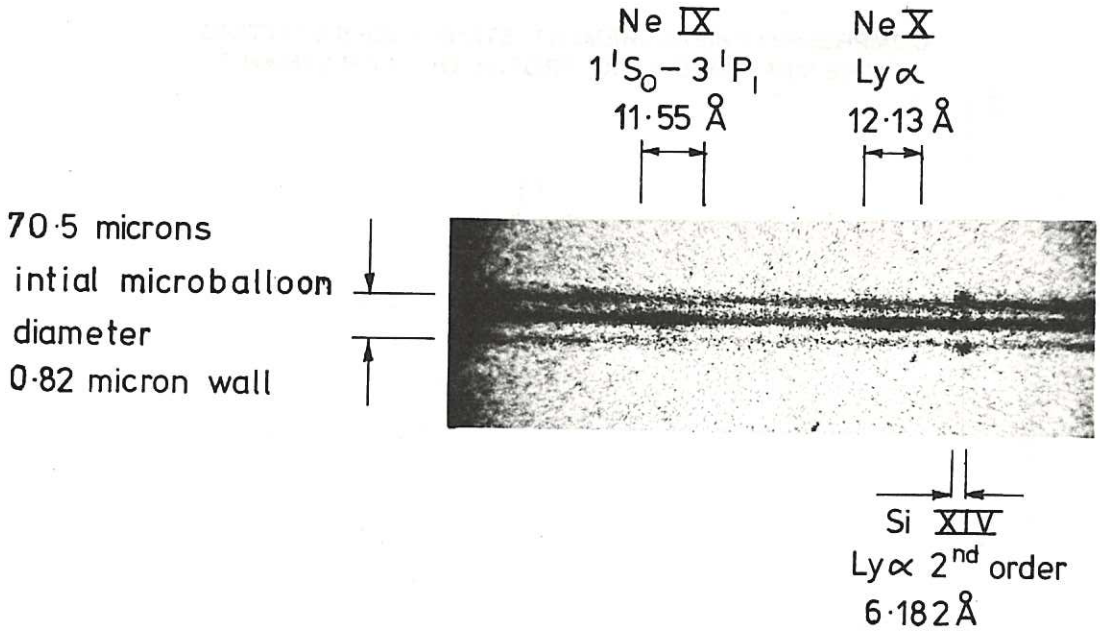

Fig.2 Space-resolved spectrum from laser-irradiated glass microballoon target filled to 8·5 bar pressure with Neon. Initial microballoon diameter is 70·5μm with wall thickness 0·82μm. The relatively narrow Si lines from the glass shell are spatially differentiated from the Stark-broadened Neon lines in the compressed core. (Rutherford Laboratory Annual Report, NOLD/78/04 – 1978).

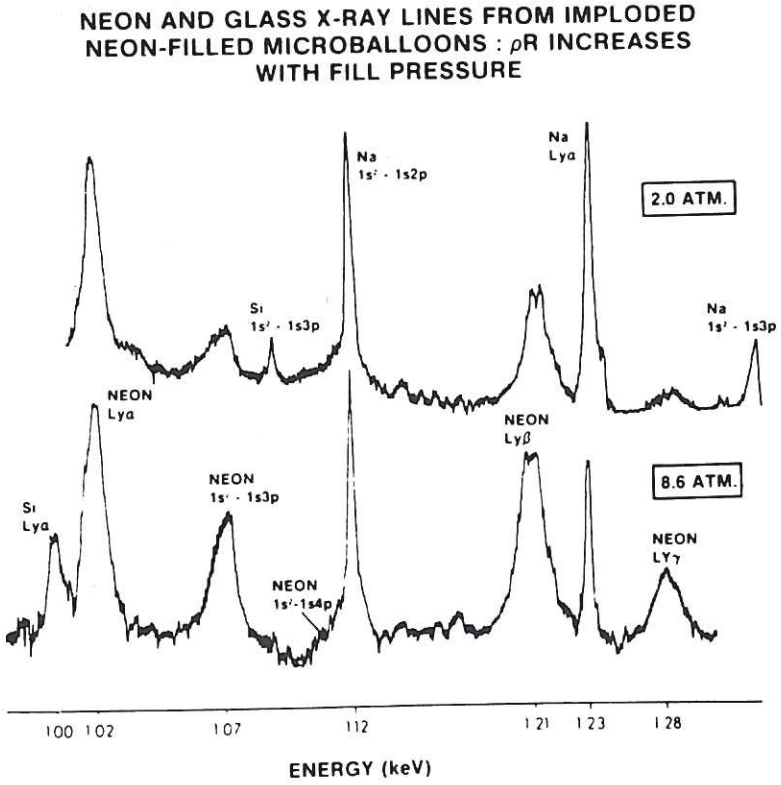

Fig.3 Microdensitometer traces of the x-ray spectrum of microballoon implosion with two different fill pressures of Neon. Sodium and Silicon lines are relatively narrow and come from the glass shell. The broader Neon lines are emitted from the compressed core. (Bristow et al [6]).

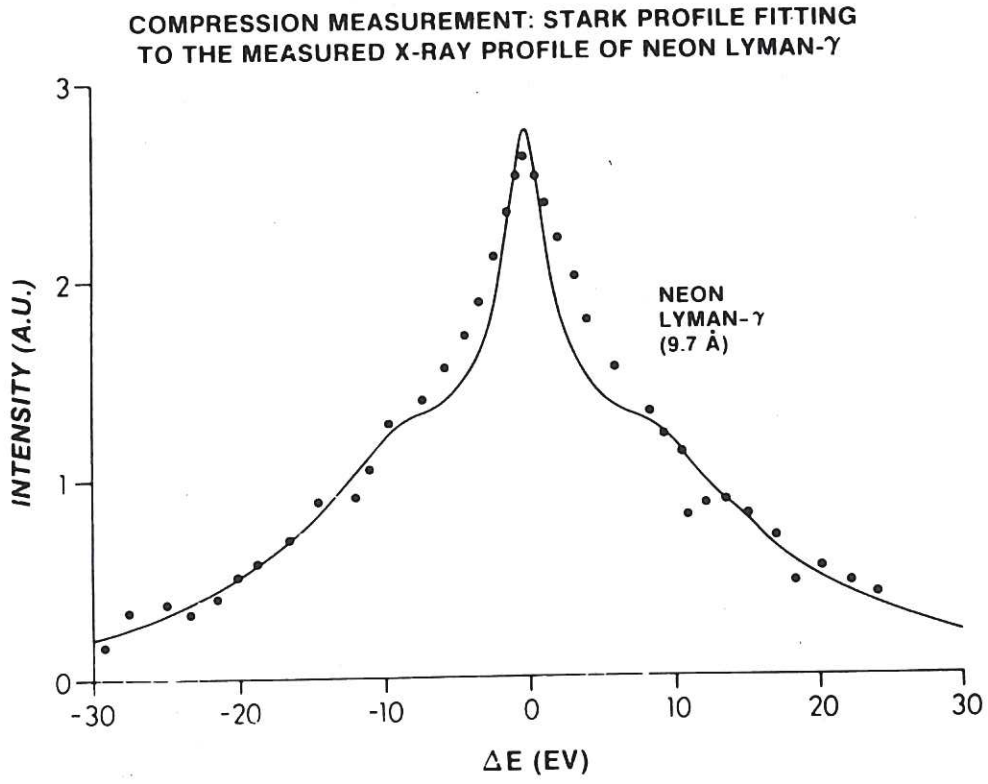

Fig.4 Theoretical profile including Stark, Doppler (Te=Ti=300eV) and instrumental broadening fitted to measured (dotted) x-ray profile emitted from core of microballoon compression. Stark profile corresponds to electron density $N_e = 7 \times 10^{22}$ cm^{-3}. (Bristow et al [6]).

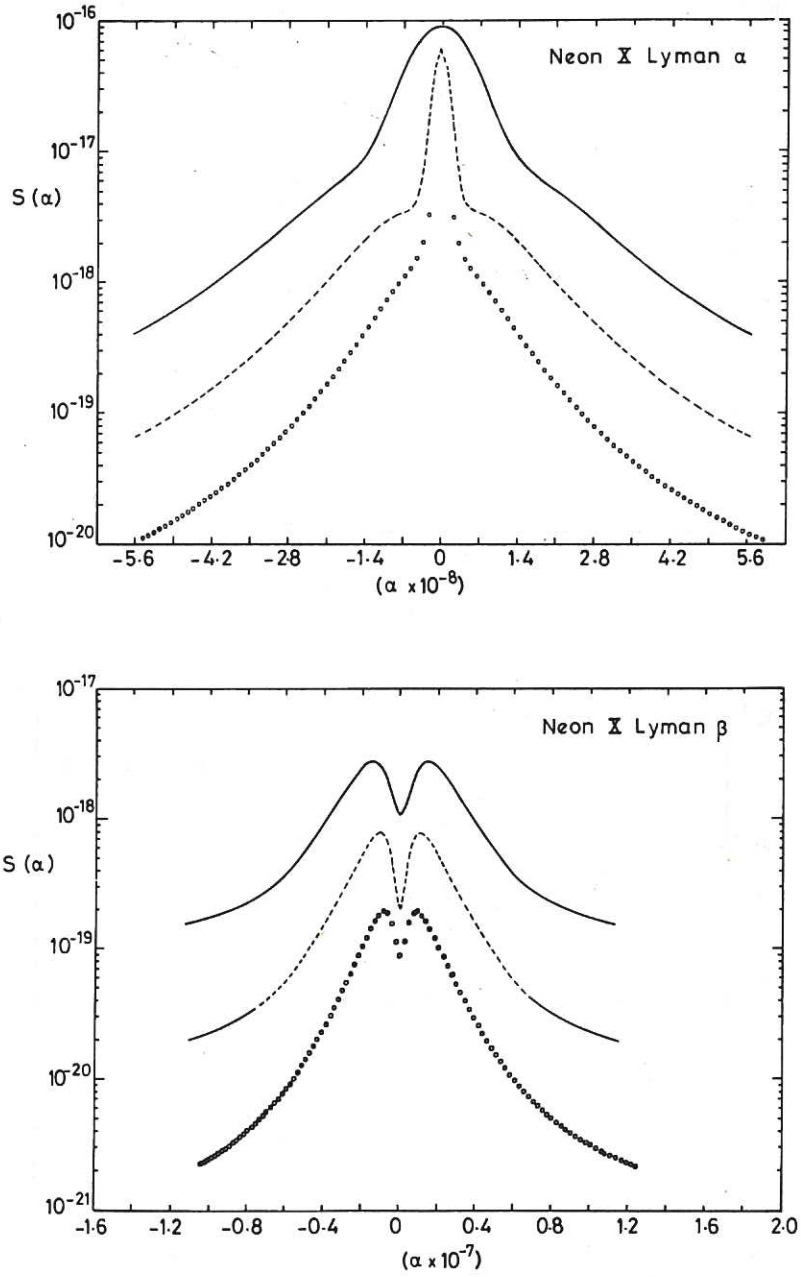

Fig.5 Theoretical Stark profiles of Neon Lyman α (upper) and Lyman β (lower) for range of electron densities, ———— represents $N_e = 5 \times 10^{21}$ cm^{-3}, - - - - - - - - - - represents $N_e = 5 \times 10^{22}$ cm^{-3}; · · · · · · · · · · represents $N_e = 5 \times 10^{23}$ cm^{-3} and $Z = Z_p = 10$. Doppler broadening for a temperature $T_e = T_i = 5 \times 10^6$ K is included. The wavelength scale may be derived from the relation $\Delta\lambda = \alpha.F_o = \alpha.2.61\ e\ N_e^{2/3}$. $S(\alpha)$ is plotted directly as the absolute absorption coefficient in cm^{-2} as a function of α. This means that the optical depth may be derived directly from $\tau(\alpha) = \rho(\text{Neon}).R.S(\alpha)$. (R.W. Lee, [27]).

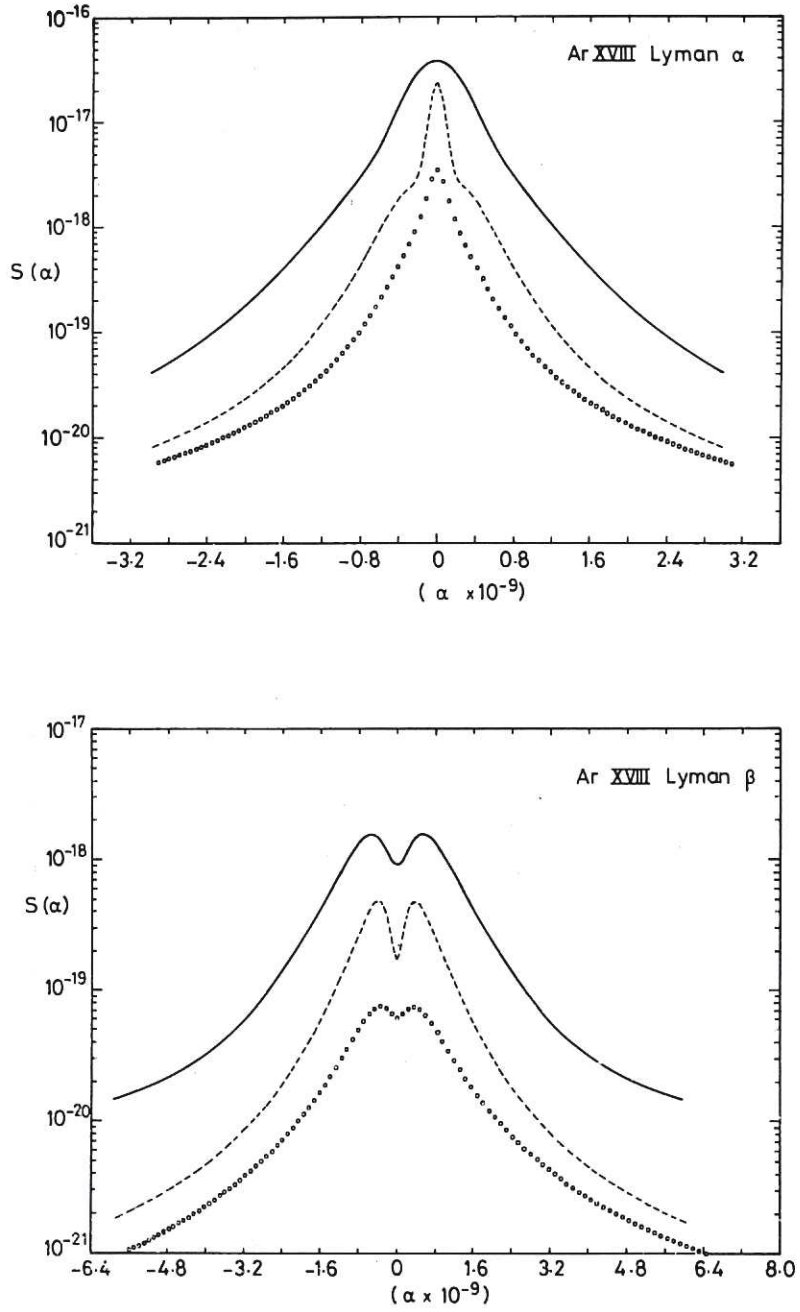

Fig.6 Theoretical Stark profiles of Argon Lyman α (upper) and Lyman β (lower) for range of electron densities, ———— represents $N_e = 5 \times 10^{22}$ cm^{-3}; - - - - - - - - - - represents $N_e = 5 \times 10^{23}$ cm^{-3}; · · · · · · · · · · represents $N_e = 5 \times 10^{24}$ cm^{-3}; and Z = 18 with $Z_p = 12$. Doppler broadening for a temperature $T_e = T_i = 5 \times 10^6$ K is included. Wavelength scale and optical depth may be derived directly as for Fig.5. (R.W. Lee [27]).

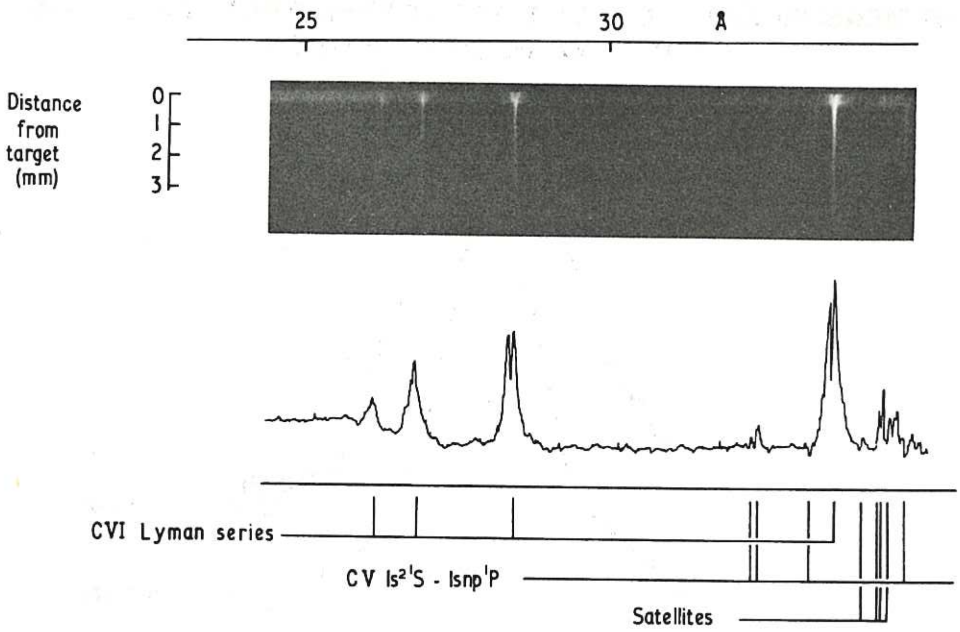

Fig.7 The Lyman spectrum of CVI in the plasma produced by laser irradiation of a polyethylene surface. The microphotometer trace shows the relative intensity of the broadened Lyman series and the adjacent free-bound continuum step. (Smith and Peacock [24]).

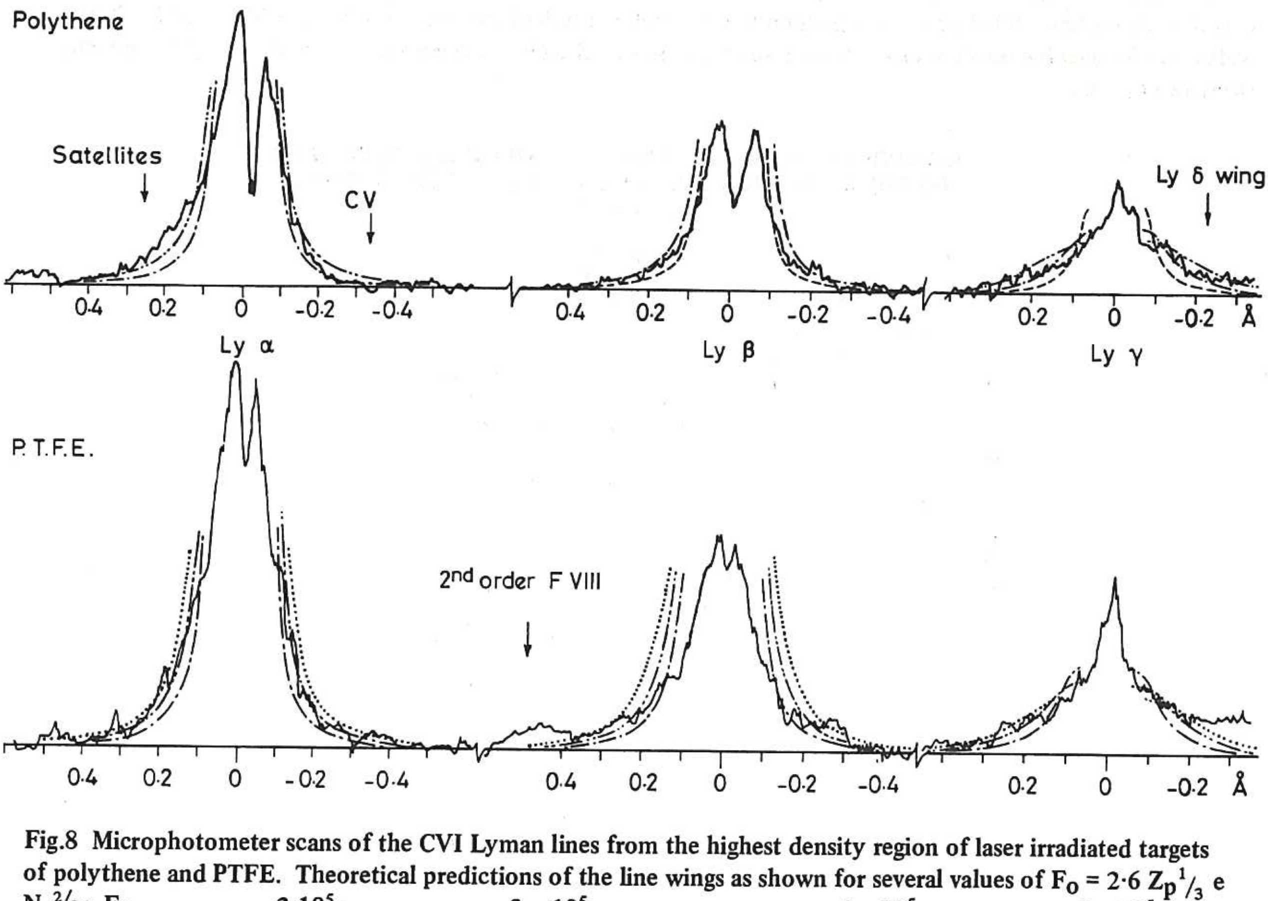

Fig.8 Microphotometer scans of the CVI Lyman lines from the highest density region of laser irradiated targets of polythene and PTFE. Theoretical predictions of the line wings as shown for several values of $F_o = 2{\cdot}6\ Z_p{}^{1}/_{3}\ e\ N_e{}^{2/3}$; Fo - - - - - - - - - - 2·10^5 ; - - - - - - - - - - - 3 x 10^5 ; - - - - - - - - - - - - - - - - 4 x 10^5 ; - - - - - - - - - - 5 x 10^5 (cgs units). The first two series members show self-reversal with peak intensities much lower due to opacity than that which would be predicted from the optical-thin line wings. For the PTFE plasma, F_o - - - - - - - - - corresponds to $N_e = 1{\cdot}3 \times 10^{21}$ cm^{-2} ; - - - - - - - - - - corresponds to $N_e = 2{\cdot}0 \times 10^{21}$ cm^{-3} ; - - - - - - - - - - - corresponds to $N_e = 2{\cdot}8 \times 10^{21}$ cm^{-3}. (Smith and Peacock [24]).

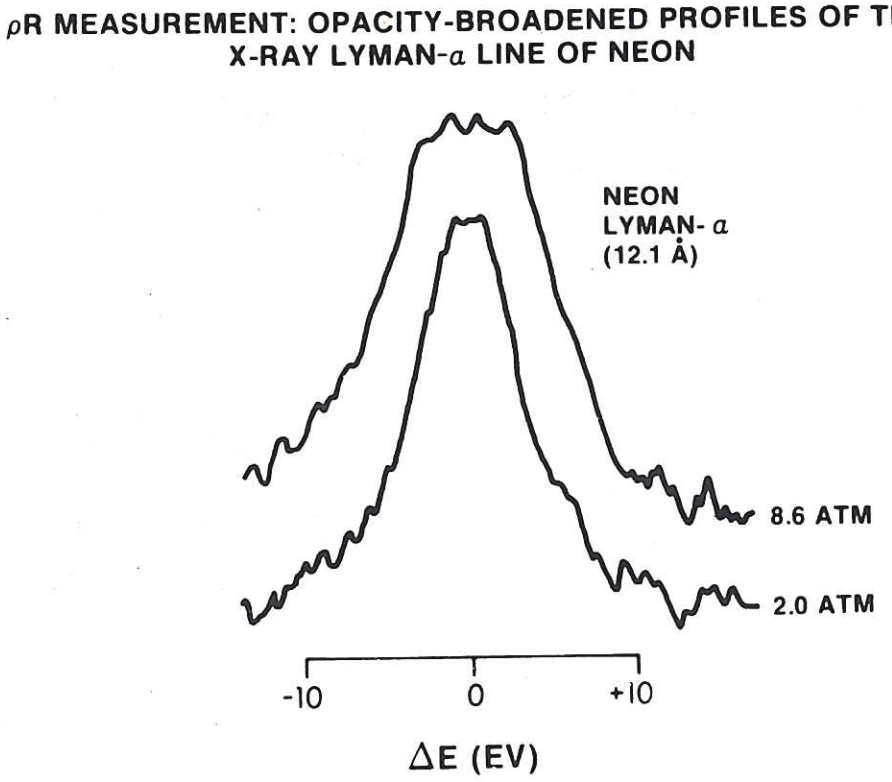

Fig.9 "Opacity-broadened" Lyman α line of NeX at 12·134 Å observed in four beam laser-irradiation experiments on Neon-filled glass microballoon target. Full width half-maxima are 7·5 and 12·0 eV while Stark width (ion broadening only), inferred from Lyman γ (Fig.4) is 5·5 eV. Derived value for $\langle \rho R \rangle = 1 \times 10^{-4}$ gm cm^{-2}. (Bristow et al [6]).

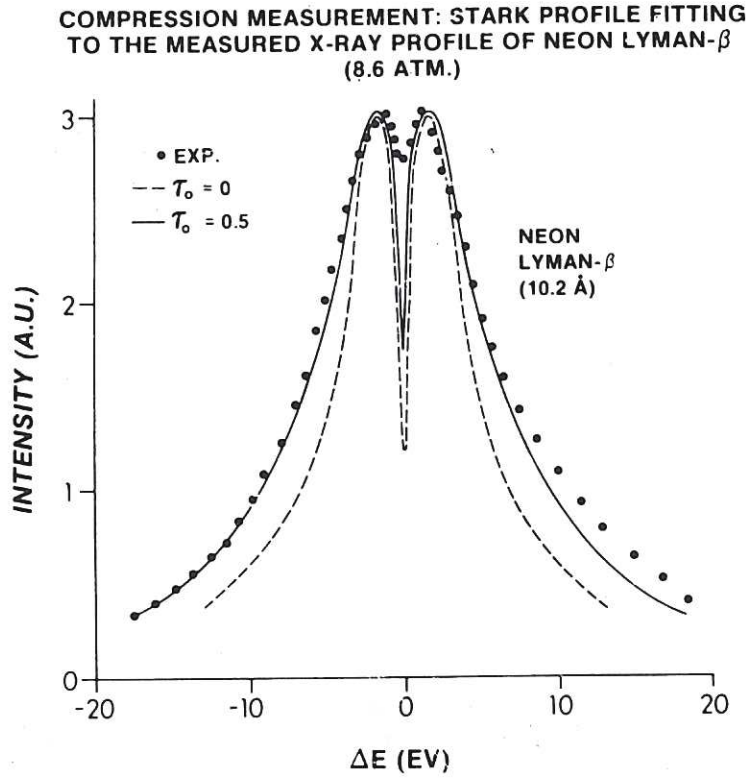

Fig.10 Fitting of theoretical and experimental (dotted) profiles of Lyman β line of Ne X from Neon-filled microballoon compression experiment. Fill pressure of Neon is 8·6 atmospheres as in Figs.4 and 9. τ_0 is the assumed optical depth at the line centre. (Bristow et al [6]).

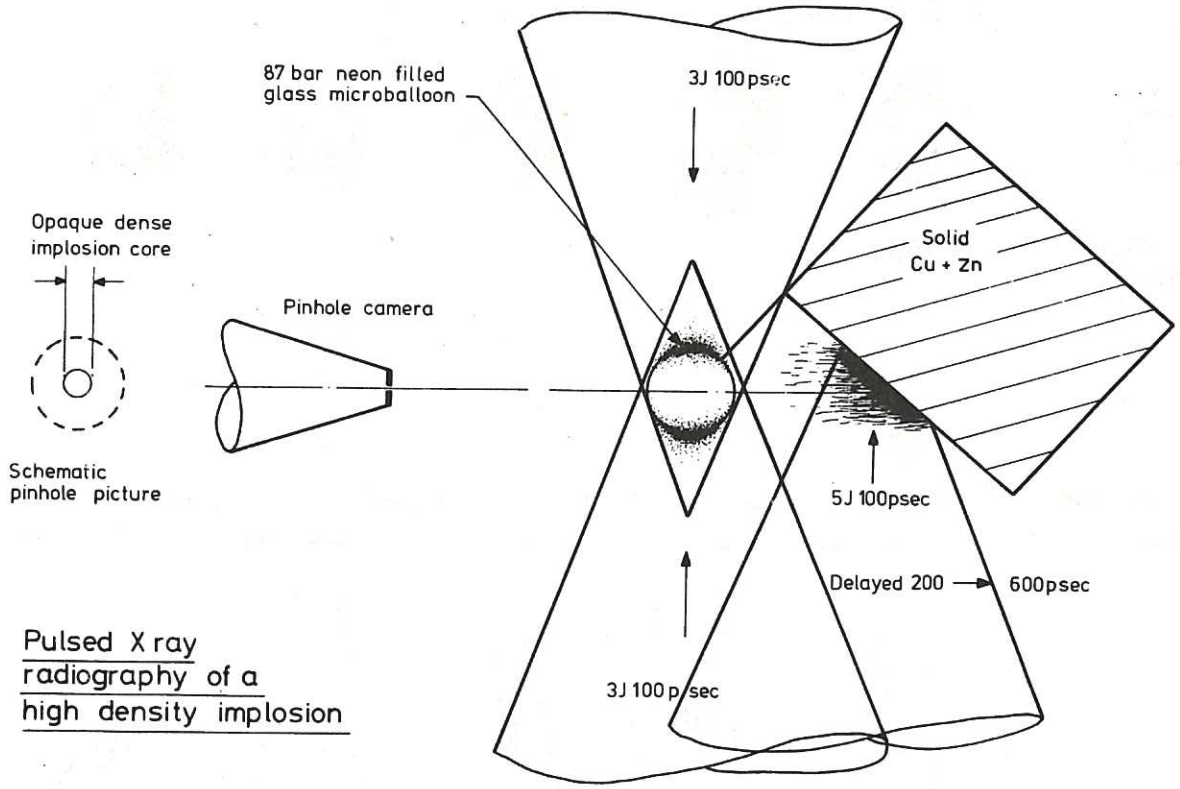

Fig.11 Lay-out of apparatus for pulsed x-ray radiography of dense compression experiment using two beams of primary irradiation. A secondary, delayed laser beam, incident on the brass target, provides a back-lit source of broad band x-ray light. (Evans et al [7]).

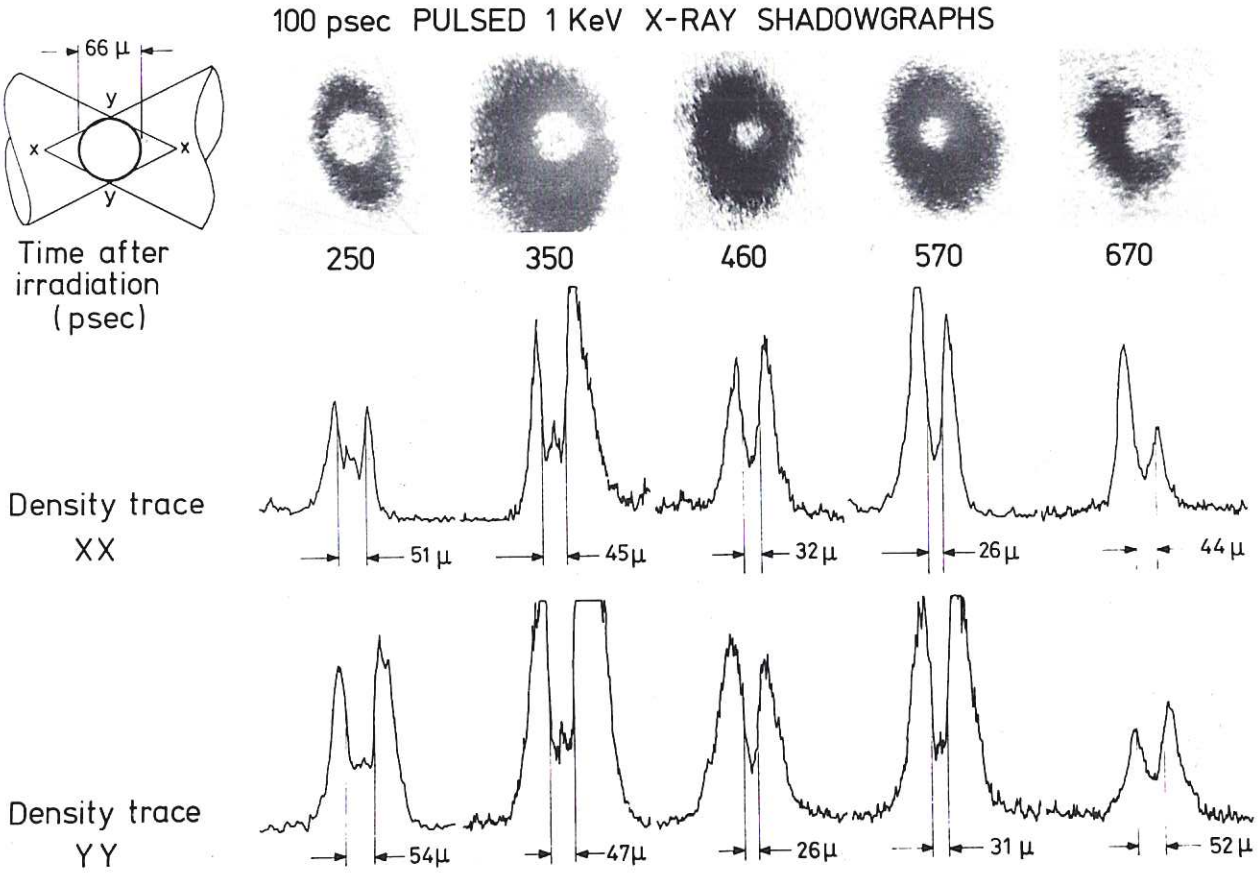

Fig.12 Composite time sequence of shadowgraphs of the compression of a high pressure gas implosion using x-ray backlighting optics as in Fig.11. (Evans et al [7]).